Slowly divergent drift in the field-driven Lorentz gas

P. L. Krapivsky and S. Redner
Center for Polymer Studies and Department of Physics, Boston University, Boston, Massachusetts 02215
(Received 3 December 1996)

The dynamics of a point charged particle that moves in a medium of elastic scatterers and is driven by a uniform external electric field is investigated. Using rudimentary approaches, we reproduce, in one dimension, the known results that the typical speed grows with time as $t^{1/3}$ and that the leading behavior of the velocity distribution is $e^{-|v|^3/t}$. In spatial dimension $d>1$, we develop an effective-medium theory that provides a simple and comprehensive description for the motion of a test particle. This approach predicts that the typical speed grows as $t^{1/3}$ for all d, while the speed distribution is given by the scaling form $P(u,t)=\langle u\rangle^{-1}f(u/\langle u\rangle)$, where $u=|v|^{3/2}$, $\langle u\rangle\sim\sqrt{t}$, and $f(z)\propto z^{(d-1)/3}e^{-z^2/2}$. For a periodic Lorentz gas with an infinite horizon, e.g., for a hypercubic lattice of scatters, a logarithmic correction to the effective-medium result is predicted in which the typical speed grows as $(t\ \ln t)^{1/3}$. [S1063-651X(97)09609-8]

PACS number(s): 02.50.−r, 05.40.+j, 05.60.+w

I. INTRODUCTION

At the turn of the century, Drude developed a qualitative theory for electrical conduction in metals [1]. To establish a more solid basis for Drude's theory, Lorentz [2] suggested an idealized model for electron transport in metals in which (i) electron-electron interactions are ignored, (ii) the background atoms are considered to be immobile spherical scatterers, and (iii) the electron-atom interaction is described by elastic scattering. This *Lorentz gas* [3] has played a large role in developing our understanding of diffusive transport in random media.

An important feature of the Lorentz gas is the independence of the electrons. This implies that the underlying Boltzmann equation for the evolution of the electron velocity distribution function (VDF) is linear. The Boltzmann equation therefore has been fruitful in understanding the properties of the Lorentz gas (see, e.g., [4] and references therein). These investigations have established that, under relatively general conditions, a test particle moves diffusively and that its diffusivity can be computed in terms of the geometric properties of the background scatterers. The Lorentz model is also simple enough to be amenable to rigorous analytical studies (see, e.g., [5–10]). In particular, for a periodic Lorentz gas in two dimensions with an ''infinite'' horizon (infinitely long straight trajectories exist), strong arguments have been given that suggest that there is anomalous diffusion of the form $\langle r^2\rangle\propto t\ \ln t$ [10]; this phenomenon is also expected to arise in arbitrary dimension.

Paradoxically, much less is known about the problem that originally motivated the Lorentz gas model, i.e., the motion of a charged test particle in a scattering medium under the influence of a spatially uniform electric field. Lorentz himself constructed a stationary solution to the Boltzmann equation by a perturbative expansion around the Maxwell-Boltzmann distribution [2]. From this solution, Lorentz reproduced the basic results of the Drude theory. Unfortunately, the starting point of Lorentz's analysis is erroneous. If the scattering is elastic (no dissipation), then an electron will necessarily gain kinetic energy as it accelerates in the field and a stationary asymptotic VDF will not exist. This dilemma motivated investigations of the field-driven Lorentz gas in which some form of dissipation is explicitly incorporated [11–13], so that it is possible to obtain Ohm's law.

In the absence of dissipation, however, Piasecki and Wajnryb [14] recognized the fundamental ramifications that arise from the nonstationarity of the system. From an exact solution to the Boltzmann equation in one dimension and an asymptotic solution for general d and with the crucial assumption of isotropic scattering, they found that (i) the root-mean-square (or typical) velocity $v_{\rm rms}$ grows with time as $t^{1/3}$ and (ii) the VDF has a nonstationary but symmetric asymptotic form whose controlling factor is $e^{-|v|^3/t}$.

Our goal in the paper is to develop simple and physically transparent approaches to understand the behavior of this field-driven Lorentz gas. We begin by considering the one-dimensional system in Sec. II, where we substantially reproduce the results of Piasecki and Wajnryb [14] by relatively simple methods. We first construct a random-walk argument to explain the mechanism that gives rise to the slow $t^{1/3}$ increase of $v_{\rm rms}$ with time. This argument relies on the assumption that each scattering event is spatially isotropic [15], a feature that we discuss in more detail later. To determine the time dependence of the speed distribution function (SDF), we employ the Langevin and underlying Fokker-Planck equations. These approaches provide a physically transparent and simple derivation of the long-time asymptotic behavior. Finally, we develop a Lifshitz argument [16] to reproduce the asymptotic tail of the SDF with minimal calculation.

In Sec. III we study the field-driven Lorentz gas for arbitrary spatial dimension d. In greater than one dimension, the freely accelerated trajectory segments between scattering events are biased by the field, leading to anisotropy in the spatial position of the test particle at the next scattering event. To account for this bias in a simple manner, we apply an effective medium approach. In this description, a particle begins at the center of a ''transparency'' sphere of radius equal to the mean free path. The particle freely accelerates until it reaches the surface of the sphere. This defines a col-

 © 1997 The American Physical Society

lision, whereupon the test particle starts at the center of a new transparency sphere. We generally assume isotropic scattering in each collision, a feature of elastic scattering from hard spheres in three dimensions [15]. However, there is actually preferential backscattering for $d<3$ and preferential forward scattering for $d>3$ [17]. Numerical simulations suggest that this short-range persistence for $d>3$ or antipersistence for $d<3$ does not affect the asymptotic motion of the test particle, so that we typically focus on isotropic scattering.

For isotropic scattering, it is simple to quantify the field-induced bias of the test particle as it moves within a transparency sphere. A random-walk argument of a similar spirit to that given in one dimension then indicates that the influence of the bias is of the same order as the stochasticity caused by scattering. This implies that the SDF will obey one-parameter scaling. From the solution to the underlying Fokker-Planck equation, we find the speed distribution $P(u,t)\propto t^{-1/2}z^{(d-1)/3}\exp(-z^2/2)$, where $u=|v|^{3/2}$ with $|v|$ the speed, and the scaling variable z is proportional to $u/t^{1/2}$. We also extend the effective-medium theory to the case where the mean free path is chosen from a distribution $\rho(\ell)\propto\ell^{-\mu}$. This allows us to investigate how the width of the mean-free-path distribution affects the transport characteristics of the Lorentz gas. As might be expected, when $\mu>3$, corresponding to a finite second moment $\langle\ell^2\rangle$ of $\rho(\ell)$, the transport of the test particle is nearly identical to the case where the mean free path is fixed. However, for $\mu<3$, i.e., for a distribution with $\langle\ell^2\rangle=\infty$, faster asymptotic transport arises. The borderline case of $\mu=3$ corresponds to a lattice array of scatterers such that an infinite horizon arises, and logarithmic corrections in the transport laws are predicted to occur, analogous to the results for the undriven Lorentz gas [18–20,10].

In Sec. IV we present Monte Carlo simulation results for test particle motion in a two-dimensional effective medium. When the radius of the transparency circle is fixed, we obtain excellent agreement between simulation results and our theoretical predictions for the case of isotropic scattering. Simulations based on the correct scattering law for hard circles in two dimensions (preferential backscattering) give virtually identical results, i.e., short-range antipersistence between trajectory segments appears to be asymptotically irrelevant. We also consider the case of a power-law distribution of radii for the transparency circle $\rho(\ell)\propto\ell^{-\mu}$. While the physically interesting case of $\mu=3$ corresponds to the borderline of applicability of our naive effective-medium approach, numerical results indicate transport properties that are close to those obtained for a fixed radius transparency circle.

In Sec. V we present a brief discussion and summary.

II. LORENTZ GAS IN ONE DIMENSION

With isotropic scattering, a test particle in a one-dimensional periodic array of scatterers undergoes an isotropic random walk as a function of the number of steps n, but with a position- and direction-dependent time increment for each hop. In the next subsection we provide a heuristic random walk argument to first determine the dependence of the typical speed on n and then infer the dependence on time. We then apply a more rigorous approach to find the SDF. As a function of n, isotropic scattering, together with the restriction of energy conservation, implies that the SDF is a half Gaussian in n. We then introduce a Langevin equation as a convenient and simple way to determine the dependence of the SDF on time.

A. Random-walk argument for the rms velocity

Consider a charged test particle that moves with constant acceleration $a=eE/m$, where e and m are the charge and mass of the particle and E is the electric field. The test particle moves in a medium of equally spaced point scatterers with separation ℓ. To mimic the behavior of a three-dimensional system with isotropic scattering, the particle hops with equal probability to its nearest neighbor on the left or the right after each collision. Thus the trajectory of the test particle consists of freely accelerating segments that are punctuated by isotropic scattering events. This is simply an isotropic random walk, but with position- and direction-dependent time increments between successive steps.

We use this picture to compute the behavior of the typical velocity as a function of time. Energy conservation gives

$$\frac{1}{2}mv_n^2-eEx_n=\text{const}, \tag{1}$$

where v_n and x_n refer to the particle velocity and position immediately after the nth scattering event. We rewrite this as

$$v_{n+1}^2-v_n^2=\frac{2eE}{m}(x_{n+1}-x_n)=\pm\frac{2eE\ell}{m}. \tag{2}$$

Because of the postulated isotropic scattering, $v_{n+1}^2-v_n^2$ is equally likely to be positive or negative. Additionally, if the particle starts at rest from $x=0$, then energy conservation implies that x cannot be negative; this provides a reflecting boundary condition at $x=0$. Thus we conclude that v_n^2 undergoes a simple random walk as a function of n, with an elementary step size given by $w^2\equiv 2eE\ell/m$, and with reflection when the velocity reaches zero. As a result,

$$\langle v_n^4\rangle\propto nw^4 \tag{3}$$

or $|v_{\rm rms}|\propto n^{1/4}w$.

To determine the dependence of $v_{\rm rms}$ on time, we write the time increment between successive collisions as

$$dt_n\equiv t_{n+1}-t_n\approx\ell/|v_n|. \tag{4}$$

The last approximation applies when the typical speed is large so that the acceleration between scatterings can be neglected. The typical elapsed time for n collisions is therefore

$$t=\sum_{k=1}^{n}dt_k\sim\frac{\ell}{w}\int_1^n\frac{dk}{k^{1/4}}\sim\frac{\ell}{w}n^{3/4}. \tag{5}$$

Solving for n as a function of time and substituting into Eq. (3) gives the fundamental result

$$v_{\rm rms}\sim w\left(\frac{wt}{\ell}\right)^{1/3}\sim(a^2\ell t)^{1/3}. \tag{6}$$

It is instructive to compare the time dependence of $v_{\rm rms}$ with that of the average velocity in the field direction. The latter can be computed from the recursion relation

$$v_{n+1} \approx \pm v_n + a dt_n \approx \pm v_n + \frac{a\ell}{|v_n|}. \tag{7}$$

By isotropy, the factor of ± 1 occurs equiprobably for each scattering and we therefore ignore the influence of the stochastic term with respect to the systematic term in Eq. (7). Since the typical speed grows indefinitely, we also ignore the acceleration during the free flight between adjacent sites, so that $v_{\rm drift} \equiv \langle v_n \rangle \approx a\ell/v_{\rm rms}$. As a function of time, this may be rewritten as

$$v_{\rm drift}(t) \sim \left(\frac{a\ell^2}{t}\right)^{1/3}. \tag{8}$$

Thus the average drift velocity *decreases* with time, even though the rms velocity increases. Therefore the VDF becomes systematically more isotropic in the long time limit [14].

Finally, using Eq. (8), one can estimate the average displacement $\langle x(t) \rangle$ in the field direction to be

$$\langle x(t) \rangle \sim v_{\rm drift}(t) t \sim (a\ell^2 t^2)^{1/3}. \tag{9}$$

Alternatively, this same result follows directly from energy conservation (1) and the time dependence of $v_{\rm rms}(t)$ from Eq. (6).

B. Speed distribution

We now derive the speed distribution using simple but rigorous approaches that obviate the need to solve the Boltzmann equation. First consider the Langevin equation to describe how the typical speed depends on n. Since v_n^2 is randomly incremented or decremented by a fixed amount w^2 in a single collision, we may write, in the large-n limit,

$$\frac{dv_n^2}{dn} = w^2 \eta(n), \tag{10}$$

where the noise has zero mean $\langle \eta(n) \rangle = 0$ and no temporal correlation $\langle \eta(n)\eta(n') \rangle = \delta(n-n')$. Since we are interested in the $n \to \infty$ limit, the continuum result for this correlation function is appropriate. In this limit, the amplitude distribution of the noise is also Gaussian. Consequently, the solution to the Langevin equation with reflection at $v_n^2 = 0$ is a half-Gaussian distribution for v_n^2 with a dispersion equal to nw^4 [21].

To determine the time dependence of the speed distribution, we transform from n to t by writing $dt = \ell\, dn/|v_n|$, so that

$$\frac{dv_n^2}{dn} = 2\ell \frac{d|v_n|}{dt}. \tag{11}$$

Next, we transform the dependence of the noise correlation from n to t. Writing $\delta(n-n') = \delta(t-t')(dt/dn)$ gives $\langle \eta(n)\eta(n') \rangle = \langle \eta(t)\eta(t') \rangle \ell/|v|$, so that $\eta(n) = \eta(t)\sqrt{\ell/|v|}$. Substituting this into the Langevin equation (10) gives

$$\frac{d|v|}{dt} = \frac{w^2}{2\ell} \sqrt{\frac{\ell}{|v|}}\, \eta(t) \tag{12}$$

or

$$\frac{d|v|^{3/2}}{dt} = \frac{3w^2}{4\sqrt{\ell}} \eta(t). \tag{13}$$

Thus we conclude that the distribution $P(u,t)$ is Gaussian in $u = |v|^{3/2}$, with a dispersion proportional to w^4/ℓ. Then the SDF is determined from the identity $P(v,t)d|v| = P(u,t)du$ to yield

$$P(v,t) = \sqrt{\frac{|v|}{4\pi\ell a^2 t}} \exp\left[-\frac{|v|^3}{9\ell a^2 t}\right]. \tag{14}$$

An independent and appealing approach to obtain the SDF is by a Lifshitz tail argument [16], in which the assumed scaling form of the SDF is matched to the "extreme" contribution that arises from a particle that is scattered in the field direction at each collision. This extreme tail can usually be estimated by elementary means, which is the basis for the appeal of this approach. Although heuristic, the advantages of this method are simplicity and wide applicability.

Our starting point is to assume that the SDF can be written in the scaling form

$$P(v,t) \sim \frac{1}{v_{\rm rms}} f(v/v_{\rm rms}), \tag{15}$$

where the scaling function $f(z)$ is expected to approach a constant as $z \to 0$ and vanish faster than any power law for $z \to \infty$. Generally, this large-z dependence is quasiexponential [22]

$$f(z) \sim \exp(-z^\delta), \tag{16}$$

where δ is the "shape" exponent of the distribution.

Consider now a trajectory in which the test particle is perpetually scattered parallel to the field, so that its speed is simply $v = at$. Substituting into Eq. (16) and using Eq. (6) for $v_{\rm rms}$ gives

$$P(v = at, t) \sim e^{-[at/(a^2\ell t)^{1/3}]^{\delta/3}} = e^{-(at^2/\ell)^{\delta/3}}. \tag{17}$$

On the other hand, the probability P_n that n scattering events are all parallel to the field equals 2^{-n}. For this uniformly accelerated motion, the correspondence between n and the time is simply $at^2/2 = n\ell$. Writing P_n as a function of time and matching with the argument of the exponential in Eq. (17) gives $\delta = 3$, in agreement with above asymptotically exact results. Note that if we define a size exponent ν through $v_{\rm rms} \sim t^\nu$, then the general scaling relation $\delta = (1-\nu)^{-1}$ [22], between the size and shape exponents, fails for the field-driven Lorentz gas.

Parenthetically, we note that the naive substitution of the dependence on the number of scattering events by the time

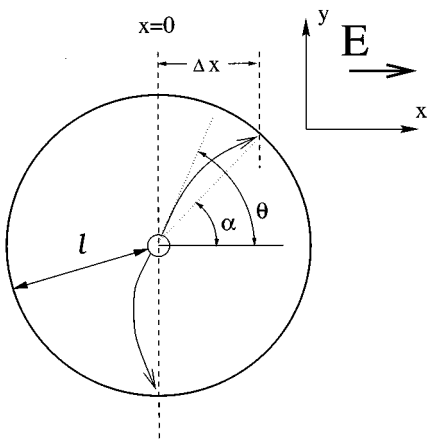

FIG. 1. "Transparency" sphere that surrounds a scatterer. After a scattering event, the test particle moves freely on a parabolic trajectory until the next collision at the sphere boundary. The initial and final angular position of the test particle θ and α, respectively, are indicated. The critical trajectory (pointing downward) is defined by the condition that the final longitudinal position of the test particle is at $x=0$.

dependence for extreme events gives a correct description for the tail of the SDF. In contrast, if we take the correct distribution of v_n^2, $P(v_n^2)\propto\exp(-v_n^4/2nw^4)$, and substitute $n\sim(wt/\ell)^{4/3}$, which expresses the average number of collisions as a function of time, we arrive at a *wrong* expression for the SDF. This suggests that the distribution of times for fixed n, averaged over all random walks, will be broad.

III. LORENTZ GAS IN GREATER THAN ONE DIMENSION

A. Effective-medium approximation

The field-driven Lorentz gas in greater than one dimension presents theoretical and computational challenges. Numerical simulations of the dissipationless system are prone to large fluctuations and quantitative conclusions are not readily obtained [11]. Because of this computational difficulty and also because dissipation arises in any physical realization of the Lorentz gas, simulations have primarily focused on the field-driven system with dissipation. This is achieved by either allowing for inelasticity in collision events [12] or introducing a "thermostat" that continuously extracts energy from the particle during its free motion to maintain a constant kinetic energy [11,23]. While much is known about these dissipative systems [23,24], our interest is in the nonstationary behavior of dissipationless system: namely, the time dependence of the typical speed and the form of the SDF.

Because of the inherent difficulties in describing the motion of a test particle in a regular lattice of scatterers, we introduce an effective-medium approximation in which the true trajectory is replaced by an effective but physically equivalent trajectory whose properties are readily calculable (Fig. 1). We assume that immediately after each scattering event, the test particle starts at the center of a transparency sphere of radius equal to the mean free path ℓ. The test particle freely accelerates until the next collision, defined to be the point where the surface of this sphere is reached. This collision point also defines the center of the next transparency sphere. This construction is repeated to generate a particle trajectory that consists of parabolic segments (the free-particle motion between collisions), which are punctuated by collision events. As discussed in the Introduction, we generally employ isotropic scattering, so that the outgoing particle direction is randomized at each collision event.

B. Typical speed

To estimate the typical speed, we need to quantify the deflection of a trajectory during free flight. Let us define trajectories whose collision points are in the hemisphere $x>0$ as positively biased and vice versa. Separating these trajectories is a "critical" trajectory, in which the next collision point is also at $x=0$ (Fig. 1). (This critical trajectory exists only if the initial speed satisfies $v>w/\sqrt{2}$; otherwise all trajectories are deflected towards increasing x. However, since the typical speed grows as a power law in time, the role of trajectories in which the speed is too small to define a critical trajectory is expected to be negligible.)

By elementary mechanics, the inclination angle of this critical trajectory is

$$\theta_c=\frac{1}{2}\sin^{-1}\left(-\frac{a\ell}{v^2}\right)\approx\frac{\pi}{2}+\left(\frac{w}{2v}\right)^2 \quad \text{as} \quad \frac{w}{v}\to 0. \tag{18}$$

Very roughly, then, we may view the longitudinal motion of the test particle as an equivalent biased one-dimensional random walk, in which trajectories with $0<\theta<\theta_c$ are mapped onto steps to the right and trajectories with $\theta_c<\theta<\pi$ are mapped onto steps to the left. From Eq. (18), the bias at each step is proportional to the inverse square of the particle speed $\epsilon=(w/2v)^2$. Following the same steps as those given in Eqs. (1)–(6), the velocity increment between scatterings is given by $v_{n+1}^2-v_n^2=\pm w^2$, but with the $\pm$ sign now occurring with respective probabilities $\frac{1}{2}(1\pm b\epsilon)$, where b is a dimension-dependent number of order unity. Thus, in addition to the stochastic particle motion given in Eq. (3), a deterministic contribution also arises. This latter component gives, for the n dependence of the speed, $v_n^2\sim n\epsilon w^2\sim nw^4/v^2$, or $|v_n|\sim n^{1/4}w$, identical to the one-dimensional result. Now employing the approach given in Sec. II A, we reproduce the same time dependence of v as in one dimension. Thus, in higher dimensions, the manifestations of isotropic scattering and field bias are of the same order in our effective-medium theory and this leads to the time dependence of the one-dimensional system.

C. Speed distribution

To determine the speed distribution, we first derive the Langevin equation for the dependence of the typical speed on n, from which the underlying Fokker-Planck equation for the SDF may be written and solved. In a time $\Delta\tau$ after collision n (and before collision $n+1$), the particle will be located at

$$\vec{r}=v\Delta\tau\hat{n}+\frac{a\Delta\tau^2}{2}\hat{e} \tag{19}$$

with respect to the center of the transparency sphere. Here $\hat{n}$ and $\hat{e}$ are the unit vectors in the direction of motion after the scattering event and the electric field, respectively, i.e., $\vec{v}_n = v\hat{n}$ and $\vec{E} = E\hat{e}$. The next collision event takes place on the surface of the sphere $\vec{r}^{\,2} = \ell^2$. Consequently, the time increment τ between collisions is implicitly given by

$$\ell^2 = (v\tau)^2 + av\tau^3(\hat{n}\cdot\hat{e}) + \frac{a^2\tau^4}{4}. \tag{20}$$

The velocity change between collisions is found from energy conservation

$$v_{n+1}^2 - v_n^2 = 2a(\vec{r}\cdot\hat{e}) = 2av\tau(\hat{n}\cdot\hat{e}) + (a\tau)^2. \tag{21}$$

Combining Eqs. (20) and (21), the time increment can be eliminated to give the analog of Eq. (2)

$$v_{n+1}^2 - v_n^2 \approx 2a\ell(\hat{n}\cdot\hat{e}) + \frac{a^2\ell^2}{v^2}[1-(\hat{n}\cdot\hat{e})^2]. \tag{22}$$

In Eq. (22) and below we ignore terms of $O(w^6/v^4)$. The first term in Eq. (22) is purely stochastic because $\langle\hat{n}\cdot\hat{e}\rangle = 0$. Since $\langle(\hat{n}\cdot\hat{e})^2\rangle = 1/d$, we may write this stochastic term as $w^2\eta(n)/\sqrt{d}$. The second term in Eq. (22) has both deterministic and stochastic components, with the magnitude of the former equal to $(a\ell/v)^2(1-1/d) = (d-1)w^4/4v^2d$, the latter being negligible in the long-time limit. Thus we obtain the Langevin equation

$$\frac{dv_n^2}{dn} = \frac{d-1}{4d}\frac{w^4}{v^2} + \frac{w^2}{\sqrt{d}}\eta(n). \tag{23}$$

In one dimension, the deterministic term disappears and Eq. (23) coincides with Eq. (10).

Following the same steps as those given after Eq. (10), we eliminate n in favor of the time to transform the above equation to

$$\frac{d|v|^{3/2}}{dt} = \frac{3(d-1)w^4}{16\ell d}\frac{1}{|v|^{3/2}} + \frac{3w^2}{4\sqrt{\ell d}}\eta(t). \tag{24}$$

In this equation, the order of magnitudes of the systematic and stochastic terms on the right-hand side are identical. Thus $|v|^{3/2}$ evolves by a biased random-walk process, but one in which the bias and the dispersion are of the same scale. This can be seen more clearly by writing the underlying Fokker-Planck equation for $P(u,t)$, where $u \equiv |v|^{3/2}$. Following the standard prescription [21], this Fokker-Planck equation is

$$\frac{\partial P}{\partial t} = \frac{9w^4}{16\ell d}\left[\frac{\partial^2 P}{\partial u^2} - \frac{d-1}{3d}\frac{\partial}{\partial u}\left(\frac{P}{u}\right)\right]. \tag{25}$$

Notice that because the bias is proportional to $1/u$, both terms on the right-hand side are of the same order and a scaling solution is appropriate. Let us therefore make the scaling ansatz

$$P(u,t) = \frac{1}{\langle u\rangle}f(z) \quad \text{with} \quad z \equiv u/\langle u\rangle. \tag{26}$$

Substituting this into the Fokker-Planck equation (25) and writing the time and velocity derivatives in terms of the scaling variable, the partial differential equation can be separated into two ordinary differential equations. From the time dependence of $\langle u\rangle$, we obtain

$$\frac{d}{dt}\langle u\rangle^2 = \frac{9w^4}{8\ell d}. \tag{27}$$

This then gives a characteristic speed that is proportional to $(w^4t/\ell)^{1/3}$ or $(a^2\ell/t)^{1/3}$. From the dependence on the scaling variable, we find that the scaling function obeys the ordinary differential equation

$$-f(z) - zf'(z) = f''(z) + \frac{d-1}{3}\left[\frac{f(z)}{z^2} - \frac{f'(z)}{z}\right], \tag{28}$$

where the prime denotes differentiation with respect to z. One integration gives

$$f'(z) = \left(\frac{d-1}{3z} - z\right)f(z) + A, \tag{29}$$

where A is a constant. Since $f(z)$ and its first derivative vanish faster than any power of z for $z\to\infty$, $A = 0$. The solution to the resulting equation is

$$f(z) = \frac{2^{(4-d)/6}}{\Gamma((d+2)/6)}z^{(d-1)/3}e^{-z^2/2}, \tag{30}$$

with $\Gamma(y)$ the gamma function [25] and the numerical coefficient is determined by the normalization condition $\int_0^\infty f(z)dz = 1$.

D. Distributed mean-free paths

In both the random-walk argument for $d = 1$ and the effective-medium theory for $d > 1$, a mean free path that has the fixed value ℓ for each scattering event was an inherent feature. However, in the Boltzmann equation approach of Piasecki and Wajnryb [14], a Poisson distribution of mean free paths is implicitly assumed. In fact, there will be a distribution of mean free paths in any real scattering medium. We therefore examine the physical effects that such a distribution has on transport properties. Probability theory [26,27] suggests that if the distribution is relatively sharp, the previous random-walk arguments apply, while for a broad distribution, different transport behavior arises. We therefore consider a power-law distribution of mean free paths

$$\rho(\ell) \sim \lambda^{\mu-1}/\ell^{\mu}, \tag{31}$$

which is expected to facilitate the absorption of field energy by the test particle for sufficiently small Lévy index μ. Additionally, this form, for $\mu = 3$, corresponds to the Lorentz gas in a scattering medium with an "infinite" horizon (e.g., a square lattice of spherical scatterers) [18–20].

Let us first consider a one-dimensional system in which a new mean free path is independently chosen from the above distribution after each scattering event. We allow μ to be arbitrary since this general situation is tractable. If the second moment of $\rho(\ell)$ is finite, i.e., $\mu > 3$, then the distribution of a

sum of a large number of independent random variables, each distributed according to $\rho(\ell)$, approaches a Gaussian and the random-walk argument of Sec. II applies. In contrast, for $\mu \leq 3$, a Lévy distribution emerges whose index depends on μ. Making use of well-known results [26,27] for Lévy distributions, we determine the n dependence of $v_{\rm rms}$ to be [the analog of Eq. (3)]

$$v_n^2 \sim w^2 \begin{cases} \sqrt{n \ln n}, & \mu = 3 \\ n^{1/(\mu-1)}, & \mu < 3, \end{cases} \tag{32}$$

with $w^2 = \lambda a$. Repeating the calculational steps employed in Sec. II, we find, for the time dependence of $v_{\rm rms}(t)$,

$$v_{\rm rms}(t) \sim w \begin{cases} \left[\dfrac{wat}{\lambda} \ln\left(\dfrac{wt}{\lambda} \right) \right]^{1/3}, & \mu = 3 \\ \left(\dfrac{wt}{\lambda} \right)^{1/(2\mu-3)}, & 2 < \mu < 3. \end{cases} \tag{33}$$

The average displacement in the field direction is thus given by $\langle x(t) \rangle = v_{\rm rms}(t)^2/2a$, while the drift velocity is $v_{\rm drift}(t) = \langle x(t) \rangle / t$. For $\mu \leq 2$, the first moment of $\rho(\ell)$ diverges, so that the typical mean free path is infinite. Consequently, collisions become irrelevant asymptotically, so that the typical velocity should grow linearly in time and an asymmetric velocity distribution should arise.

IV. NUMERICAL SIMULATIONS

To test our theoretical predictions, we perform Monte Carlo simulations of particle motion in a two-dimensional effective medium. An important element in this simulation is determining where an arbitrary parabolic trajectory, which starts at the origin, intersects the circumference of a concentric circle. This involves the unwieldy solution of a quartic equation. However, since the typical speed grows with time, individual trajectory segments should be only slightly curved in the long-time limit. Thus we compute the trajectory and the time between collisions in a perturbation series appropriate for the large speed limit. If the speed happens to fall below a preset threshold such that a strongly curved trajectory segment should arise, we impose the constraint that for this segment the particle is deflected exactly parallel to the field. We anticipate that this "reflecting" boundary condition in velocity space has a negligible influence on the long-time motion of the test particle.

Our simulation algorithm therefore consists of the following steps to compute the velocity and time increments between collisions. These steps are repeated to generate a single-particle trajectory.

(i) If the speed is above a predetermined threshold $v_{\rm th}$, then:

(a) Choose a random scattering angle in the range $0 \leq \theta \leq \pi$ (see Fig. 1).

(b) Determine the angular position α of the particle when it hits the surface of the circle. From elementary mechanics, α is perturbatively given in the large velocity limit by

$$\alpha = \theta - \epsilon \sin\theta + \epsilon^2 \sin 2\theta + \cdots,$$

with $\epsilon = (w/2v)^2$.

(c) From the angle α, determine the change in the longitudinal position of the particle Δx and thereby determine the change in the speed of the particle by $v_f^2 = v_i^2 + w^2 \Delta x/\ell$. Here v_i is the velocity of the particle as it begins from the center of the transparency circle and v_f is the particle velocity just before the collision at the circumference of the circle.

(d) Determine the time increment τ associated with this trajectory. In the large velocity limit, τ is perturbatively given by

$$\tau = \frac{\ell}{|v|} \left\{ 1 - \epsilon \cos\theta + \frac{5\epsilon^2}{2} (\cos^2\theta - 1) + \cdots \right\}.$$

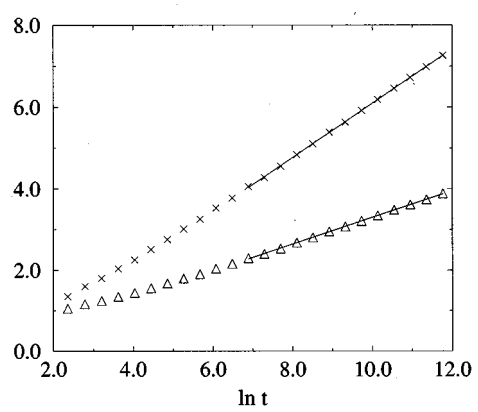

FIG. 2. Monte Carlo simulation results for 2000 walks of 1.5^{29} steps in a two-dimensional effective medium. Shown are $v_{\rm rms}(t)$ (△) and the mean longitudinal position $\langle x(t) \rangle$ (×). The straight lines represents the best fits to the data in the range $1.5^{17} \leq t \leq 1.5^{29}$.

(ii) If the speed is less than $v_{\rm th}$, then, the scattering angle is taken to be $\theta = 0$. Consequently, $v_f^2 = v_i^2 + w^2$ and $\tau = 2\ell/(|v_i| + |v_f|) \approx 2\ell/w$.

Clearly, the different particle update rules for initial speed smaller or larger than the threshold is a crude approximation. One can envision more accurate but more cumbersome rules to integrate over low-speed trajectory segments. Since these segments are relatively unlikely, this refinement was not pursued and indeed appears to be unnecessary. Also, because of the arbitrariness in the integration over the low-speed segments, the actual value of $v_{\rm th}$ is also somewhat arbitrary and we chose $v_{\rm th} = w$. To appreciate the role of trajectory curvature, note that when $v = v_{\rm th}$ the maximum deviation between the initial and final angular positions of the trajectory arises when $\theta \approx 111.5°$, with $\alpha - \theta \approx -15.8°$. For $v = 2v_{\rm th}$, the maximum deviation point occurs when $\theta \approx 97°$, with $\alpha - \theta \approx -3.7°$. Thus the effect of curvature in the individual trajectory segments is typically small.

Typical results from this Monte Carlo simulation with isotropic scattering are presented in Fig. 2. Shown are $v_{\rm rms}(t)$ and $\langle x(t) \rangle$ on a double logarithmic scale based on 2000 trajectories of $1.5^{29} \approx 127\,834$ steps for the case where the transparency circle has a fixed radius. After some transient

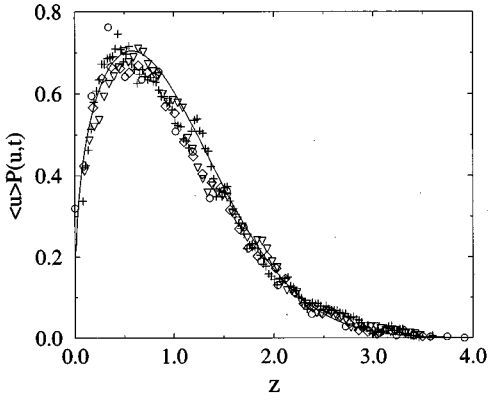

FIG. 3. Scaled distribution $f(z)\equiv\langle u\rangle P(u,t)$ versus $z\equiv u/\langle u\rangle$, where $u=|v|^{3/2}$. Representative data shown include $t=1.5^{20}$ (○) and $t=1.5^{23}$ (◇) smoothed over a three-site neighborhood, $t=1.5^{26}$ (▽) smoothed over a five-site neighborhood, and $t=1.5^{29}$ (+) smoothed over a seven-site neighborhood. The curve is the theoretical prediction $0.930\cdots\times z^{1/3}e^{-z^2/2}$.

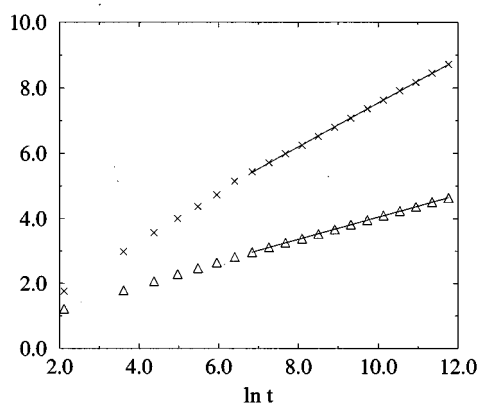

FIG. 4. Monte Carlo simulation results for 2000 walks of 1.5^{29} steps in a two-dimensional effective medium in which the radius ℓ of the transparency sphere is drawn from the distribution $\rho(\ell)\propto\ell^{-3}$. Shown are $v_{\rm rms}(t)$ (△) and the mean longitudinal position $\langle x(t)\rangle$ (×). The straight lines represents the best fits to the data in the range $1.5^{17}\leq t\leq 1.5^{29}$.

behavior, the data for $t\gtrsim 500$ appear to be linear and a linear least-squares fits yields the respective slopes of 0.329 and 0.665, in excellent agreement with the respective theoretical predictions of 1/3 and 2/3.

In Fig. 3 we present corresponding results for the distribution of $u=|v|^{3/2}$ at $t=1.5^{20}$, $t=1.5^{23}$, $t=1.5^{26}$, and $t=1.5^{29}$. The raw data has been scaled so that the abscissa is $z=u/\langle u\rangle$, while the ordinate is $f(z)=\langle u\rangle P(u,t)$. This scaled data at later times have then been smoothed by averaging over a small neighborhood to reduce fluctuations. These data compare well with the theoretical prediction $f(z)=[2^{1/3}/\Gamma(2/3)]z^{1/3}e^{-z^2/2}$ (Fig. 3).

We also performed a more faithful simulation for two dimensions in which the correct hard-circle scattering is implemented. In place of step (i) given above, we assume that just before the nth collision, with incidence angle α_{n-1} (see Fig. 1), the test particle uniformly illuminates the cross section of the scatterer, which is taken to be a circle of radius r. After specular reflection by the scatterer, the difference between the incident and final angles is $d\psi=\pi-2\sin^{-1}(b/r)$, where the impact parameter b is uniformly distributed between $\pm r$. This angular deflection is used to compute the outgoing angle $\theta_n=\alpha_{n-1}+d\psi$ and the corresponding incoming angle α_n. Our simulation results for this more faithful implementation of hard-circle scattering are virtually identical to those from isotropic scattering and give the exponent estimates of 0.330 and 0.662 for the time dependence of $v_{\rm rms}(t)$ and $\langle x(t)\rangle$, respectively. Because of this agreement, and also for simplicity, our simulations concentrated on the case of isotropic scattering.

As discussed previously, a lattice array of scatterers leads to a power-law distribution of mean free paths. We therefore also performed simulations of the effective medium when the radius of the next transparency circle is chosen from the distribution $\rho(\ell)\sim\lambda^{\mu-1}/\ell^{\mu}$, with $\mu=3$. We find that the time dependence of $v_{\rm rms}(t)$ and $\langle x(t)\rangle$ is quite close to that obtained for the case of a fixed-radius transparency circle. After a relatively long transient, the data for $t\gtrsim 1000$ appear to be linear on a double logarithmic scale and a linear least-squares fits in this range yield the respective slopes of 0.340 and 0.671 (Fig. 4). The data for $v_{\rm rms}(t)$ and $\langle x(t)\rangle$ exhibit a slight downward trend, a feature that could be attributed to a logarithmic correction. However, our data are insufficient to test for such a correction quantitatively. The distribution of speeds also exhibits relatively good data collapse, but there are quantitative discrepancies between the shape of the scaling function and the prediction $f(z)\approx 0.930\cdots\times z^{1/3}e^{-z^2/2}$ that fit the data for the case of a fixed-radius transparency sphere (Fig. 5).

V. DISCUSSION AND SUMMARY

We have investigated the motion of a charged particle that is driven by a constant field in a dissipationless elastic and isotropic scattering medium: the field-driven Lorentz gas. A fundamental aspect of this system is that the transport is nonstationary so that the typical velocity grows with time as

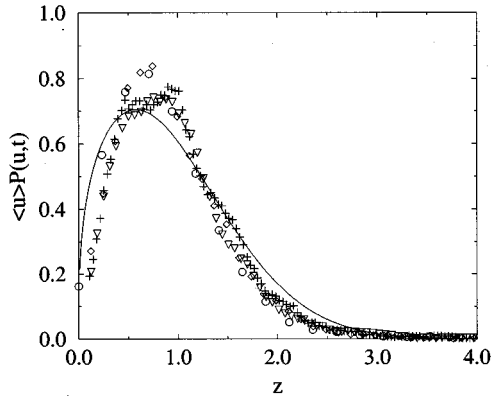

FIG. 5. Scaled distribution $f(z)=\langle u\rangle P(u,t)$ versus the variable $z\equiv u/\langle u\rangle$, where $u=|v|^{3/2}$. The radius ℓ of the transparency sphere is drawn from the distribution $\rho(\ell)\propto\ell^{-3}$. Representative data shown include $t=1.5^{20}$ (○) and $t=1.5^{23}$ (◇) smoothed over a three-site neighborhood, $t=1.5^{26}$ (▽) smoothed over a five-site neighborhood, and $t=1.5^{29}$ (+) smoothed over a seven-site neighborhood. The curve is $0.930\cdots\times z^{1/3}e^{-z^2/2}$.

$t^{1/3}$. Although this growth is unbounded, it is significantly slower than the linear time dependence that would occur in the absence of scattering. In one dimension, we have developed a random-walk description that involves isotropic hopping together with a position- and direction-dependent time increment for each hop that correctly predicts the anomalous time dependence of the typical velocity and mean displacement.

Based on this random-walk picture, we obtained the velocity distribution by writing first the Langevin equation for the typical velocity and then the underlying Fokker-Planck for the velocity distribution. We also constructed a Lifshitz tail argument that reproduced the correct behavior for the velocity distribution. The solution to the Fokker-Planck equation yields the Gaussian distribution in the variable $u=|v|^{3/2}$,

$$P(u,t)\propto\frac{1}{\sqrt{t}}e^{-u^2/t}, \tag{34}$$

which, when written in terms of $|v|$, becomes

$$P(v,t)\propto\sqrt{\frac{|v|}{t}}\,e^{-|v|^3/t}. \tag{35}$$

Interestingly, this is similar but not coincident with the asymptotic velocity distribution function

$$P(v,t)\propto\frac{1}{t^{1/3}}e^{-|v|^3/t} \tag{36}$$

obtained by Piasecki and Wajnryb [14] from the Boltzmann equation. However, their approach implicitly assumes an ''annealed'' medium with a Poisson distribution of distances between collisions. While our random walk and the Boltzmann approach should give the same scaling of the typical speed with time, the form of the velocity distribution from the two approaches should not be expected to coincide.

Our random-walk argument can also be applied to the interesting case of an alternating electric field $E(t)=E_0\sin(\omega t)$ and gives the counterintuitive result that the combination of an ac field and isotropic scattering leads to unbounded growth in the speed. This growth arises because of the isotropy in the scattering events. When the time between collisions becomes less than the time for the field to reverse, then the direction of the field becomes irrelevant. Consequently, our random-walk argument for a dc field directly applies and $v_{\rm rms}$ should grow as $t^{1/3}$. Thus scattering assists in the absorption of field energy by the test particle in an ac field, while with no scattering, a test particle merely follows the field and the typical speed is bounded.

In higher dimensions, we introduced an effective-medium approximation that provides a physically appealing description for the motion of a charged test particle. This approximation posits that the test particle moves on a parabolic field-biased trajectory within a ''transparency'' sphere and that an isotropic collision event occurs when the particle reaches the surface of this sphere. The assumption of scattering when a particle moves a fixed radial distance implies an annealed medium. Thus one might anticipate that there could be a direct connection between the effective-medium and the Boltzmann equation approaches. Because of the bias in the free-particle trajectory segments, the isotropy in outgoing particle directions immediately after one scattering event becomes anisotropic at the next scattering. Within an equivalent one-dimensional random-walk description of the test particle motion, this anisotropy can be described in terms of an effective bias that is proportional to $1/v^2$. The logical consequences of this feature again leads to a typical speed that again grows as $t^{1/3}$, just as in one dimension.

The effect of the field-induced bias is more apparent in the behavior of the speed distribution. Following a similar approach to that given for one dimension, the solution to the Fokker-Planck equation for $u=|v|^{3/2}$ is

$$P(u,t)\propto\frac{1}{\sqrt{t}}\left(\frac{u}{\sqrt{t}}\right)^{(d-1)/3}e^{-u^2/t}, \tag{37}$$

which when written in terms of $|v|$ gives

$$P(v,t)\propto\frac{|v|^{d/2}}{t^{(d+2)/6}}e^{-|v|^3/t}, \tag{38}$$

while the corresponding result of Piasecki and Wajnryb is

$$P(v,t)\propto\frac{|v|^{d-1}}{t^{d/3}}e^{-|v|^3/t}. \tag{39}$$

While these two forms agree for $d=2$, the coincidence seems fortuitous. The Boltzmann approach explicitly builds in isotropy in the collision events and in the intervening particle motion, while the effective medium explicitly accounts for the field-induced bias between scattering events.

An attractive aspect of the effective-medium approach is that it can be easily generalized to a distribution of mean free paths, a feature that arises in a lattice realization of the Lorentz gas. Such a distribution may be accounted for by a power-law distribution of sphere radii $\rho(\ell)\propto\ell^{-\mu}$, with $\mu=3$. This represents a marginal case between the regime where distributed radii appear to have no effect, for $\mu>3$, to the case where the scaling of the mean speed with time is affected, for $2<\mu<3$. Our numerical simulations indicate that the case of $\mu=3$ leads to behavior similar to that of no dispersion in the sphere radii. However, the applicability of either the Boltzmann equation approach or our effective-medium description to a lattice realization of the Lorentz gas has yet to be tested.

ACKNOWLEDGMENTS

We thank R. S. Chivukula for a helpful discussion and J. Machta for particularly useful advice about hard-sphere scattering and related suggestions. This research was supported in part by the NSF (Grants Nos. DMR-9219845 and DMR-9632059) and by the ARO (Grant No. DAAH04-93-G-0021).

[1] P. Drude, Ann. Phys. (Leipzig) **1**, 566 (1900); **3**, 369 (1900).
[2] H. A. Lorentz, Arch. Neerl. **10**, 336 (1905) [reprinted in *Collected Papers* (Nijhoff, The Hague, 1936), Vol. III, p. 180].
[3] Sometimes the Lorentz gas is called a Galton board; see, e.g., M. Kac, Sci. Am. **211** (3), 92 (1964).
[4] E. H. Hauge, in *Transport Phenomena*, edited by G. Kirczenow and J. Marro, Lecture Notes in Physics Vol. 31 (Springer-Verlag, Berlin, 1974), p. 337.
[5] L. A. Bunimovich and Ya. G. Sinai, Commun. Math. Phys. **78**, 247 (1980); **78**, 479 (1981).
[6] J. Machta and R. Zwanzig, Phys. Rev. Lett. **50**, 1959 (1983).
[7] B. Friedman and R. F. Martin, Phys. Lett. **105A**, 23 (1984); Physica D **30**, 219 (1988).
[8] J. Machta and B. Reinhold, J. Stat. Phys. **42**, 949 (1986).
[9] L. A. Bunimovich, Ya. G. Sinai, and N. I. Chernov, Russ. Math. Surv. **46**, 47 (1991).
[10] P. Bleher, J. Stat. Phys. **66**, 315 (1992).
[11] B. Moran, W. G. Hoover, and S. Bestiale, J. Stat. Phys. **48**, 709 (1987).
[12] A. Lue and H. Brenner, Phys. Rev. E **47**, 3128 (1993).
[13] N. I. Chernov, G. L. Eyink, J. L. Lebowitz, and Ya. G. Sinai, Phys. Rev. Lett. **70**, 2209 (1993).
[14] J. Piasecki and E. Wajnryb, J. Stat. Phys. **21**, 549 (1979).
[15] L. D. Landau and E. M. Lifshitz, *Mechanics* (Pergamon, Oxford, 1976).
[16] I. M. Lifshitz, S. A. Gredeskul, and L. A. Pastur, *Introduction to the Theory of Disordered Systems* (Wiley, New York, 1988).
[17] An elementary geometric consideration gives $2^{-(d-1)/2}$ for the probability of backscattering from a sphere in d dimensions; $2^{-(d-1)/2}>1/2$ when $d<3$ and thus in low dimensions backscattering indeed prevails.
[18] L. A. Bunimovich, Zh. Eksp. Theor. Fiz. **89**, 1452 (1985) [Sov. Phys. JETP **62**, 842 (1985)].
[19] J.-P. Bouchaud and P. Le Doussal, J. Stat. Phys. **41**, 225 (1985).
[20] A. Zacherl, T. Geisel, J. Nierwetberg, and G. Radons, Phys. Lett. **114A**, 317 (1986).
[21] N. G. Van Kampen, *Stochastic Processes in Physics and Chemistry* (North-Holland, Amsterdam, 1984).
[22] M. E. Fisher, J. Chem. Phys. **44**, 616 (1966).
[23] D. J. Evans and G. P. Morriss, *Statistical Mechanics of Nonequilibrium Liquids* (Academic, London, 1990).
[24] N. I. Chernov, G. L. Eyink, J. L. Lebowitz, and Ya. G. Sinai, Commun. Math. Phys. **154**, 569 (1993).
[25] *Handbook of Mathematical Functions*, edited by M. Abramowitz and I. A. Stegun (Dover, New York, 1965).
[26] B. V. Gnedenko and A. N. Kolmogorov, *Limit Distributions for Sums of Independent Random Variables* (Addison-Wesley, Reading, MA, 1954).
[27] J.-P. Bouchaud and A. Georges, Phys. Rep. **195**, 127 (1990).